International Journal of Earth, Energy and Environmental Sciences
ISSN: 2517-942X
Vol:1, No:8, 2007

The Pixel Value Data Approach for Rainfall Forecasting Based on GOES-9 Satellite Image Sequence Analysis

C. Yaiprasert, K. Jaroensutasinee, and M. Jaroensutasinee

***Abstract*—**To develop a process of extracting pixel values over the using of satellite remote sensing image data in Thailand. It is a very important and effective method of forecasting rainfall. This paper presents an approach for forecasting a possible rainfall area based on pixel values from remote sensing satellite images. First, a method uses an automatic extraction process of the pixel value data from the satellite image sequence. Then, a data process is designed to enable the inference of correlations between pixel value and possible rainfall occurrences. The result, when we have a high averaged pixel value of daily water vapor data, we will also have a high amount of daily rainfall. This suggests that the amount of averaged pixel values can be used as an indicator of raining events. There are some positive associations between pixel values of daily water vapor images and the amount of daily rainfall at each rain-gauge station throughout Thailand. The proposed approach was proven to be a helpful manual for rainfall forecasting from meteorologists by which using automated analyzing and interpreting process of meteorological remote sensing data.

***Keywords*—**Pixel values, satellite image, water vapor, rainfall, image processing.

I. Introduction

METEOROLOGICAL satellite data have been operational in weather services for more than 30 years. During this period, forecasting of severe weather based on satellite remote sensing data has been a challenging task [4]-[6]. Early warnings of severe weather, made possible by timely and accurate forecasting will help prevent casualties and damage caused by natural disasters. This is particularly significant and urgent in Thailand, where has so often suffered from flooding due to inadequate flood controls, preventions and mitigations in the country.

For example, at least 176 people died and more than 450,000 were homeless or in hardship following the severe flooding that engulfed northern Thailand after Typhoon Usagi swept through the area in August, 2001. The worst affected area had been the Lom Sak district in the mountainous north-central province of Phetchabun. Massive mudslides tore down the mountainside in the early hours of August 11, uprooting vegetation and burying seven villages with more than two meters of water and mud. Since almost all flash floods are caused by intensive heavy rainfall, the responsible authorities have a key and clear mandate to provide both accurate and advanced forecasting of possible heavy rainfall [1]-[3].

Meanwhile, detail study of water vapor quantity in the atmosphere remains a challenge and an important issue for the meteorological community. These flash flooding phenomena are often caused by severe weather such as heavy rainfalls, thunderstorms and hurricanes [7]-[10].

In order to improve the current measures of severe flood controls in Thailand, it is necessary to accurately predict and/or gather the amount of rainfall in order to be able to determine the possibility of excess amount of water in stream causing flash flooding. However, it is not practical to install a vast number of automatic rainfall sensors throughout the hot spots in the montanes that can transmit these rainfall information to achieve the measures. It is then desirable to look for a continuous source of weather information and the meteorological satellites can provide such information. Therefore, it would be of urgent task to determine the amount of rainfall and correlate these quantities to water vapor satellite data by using image processing technique over Thailand region [11]-[15]. A meteorological analysis of all Pixel Value Index (PVI) can be performed by taking into account their corresponding environmental, physical variables to the ground, such as temperature, wind divergence and water vapor flux divergence. As a result, the correlations and causalities between the PVI technique and heavy rainfall occurrences can be deduced from the historical remote sensing scenarios and it can be represented as knowledge assisting to predict potential occurrences of heavy precipitation.

Unfortunately, meteorologists continue to manually track, characterize and analyze air dynamic systems using so-called expert-eye-scanning technique. The meteorologists carry out extensive manual work to discover the moving trajectories and devolvement trends of air dynamic systems from the satellite remote sensing images. They use professional experience and knowledge [16]. However, the volumes of satellite image data

Manuscript received October 15, 2007. This work was supported in part by TOTAL Foundation and TOTAL E&P Thailand, TRF/Biotec special program for Biodiversity Research Training grant BRT T_550001, Commission on Higher Education, and CXKURUE, the Institute of Research and Development, Walailak University.

C. Yaiprasert, K. Jaroensutasinee and M. Jaroensutasinee are with Complex System Research Unit and Computational Science Graduate Program, Walailak University, Thaiburi, Thasala, Nakhon Si Thammarat, 80161, Thailand (e-mails: a.cirrus@gmail.com, krisanadej@gmail.com, and jmullica@gmail.com).

can be huge, making this method inadequate for tracking air dynamic systems covering wide ranges and long time periods. The method is time consuming, ineffective and often yields unstable and variable results from the different experts involved, it is affecting the reliability of heavy rainfall forecasting.

To address the above problems, this paper aims to provide meteorologists with an automatic spatial data method based on PVI technique and analysis in the satellite image sequence with possible heavy rainfall. It can be predicted so that effective flood control measures can be taken. The basic principle behind the method is to formulate from a recent collection data that the movement and propagation of water vapor dynamic systems over the west Pacific region. It is the crucial factor leading to the heavy rainfall in Thailand. The method used is data mining and knowledge discovery techniques. Firstly, the image sequences of water vapor map acquired from the Geostationary Meteorological Satellite (GMS) were used. The qualified of PVI was automatically identified by image processing and high computing techniques.

The rest of this paper is organized as follows: Firstly, in Section 2, the satellite data sources used in the study are introduced. Section 3 presents a methodology of the PVI image processing techniques. The experimental results are illustrated in Section 4. Finally, concluding remarks are provided in Section 5.

II. Data Sources

Satellite images have been used extensively to study temporal changes. Information and knowledge of water vapor dynamic systems are crucial to heavy rainfall forecast the collection of large amounts of satellite data with high spatial and temporal resolutions is indispensable [17], [18]. For this purpose, satellite remote sensing images of the water vapor data, taken by the GOES-9 satellite, and data of the number of rainfall were provided by the Thailand Meteorology Department (TMD) for use in this study. The data covers the time period from January to December 2004, a representative period when the Thailand suffered from intensive heavy rainfall.

The meteorological satellite, GOES-9 image is one of a new series of advanced geostationary sensors with improved infrared spatial resolution and radiometric sensitivity [19]. GOES-9 has been placed in a geosynchronous orbit at 155° E since 23 May 1995 and started its operational observation over the west Pacific region on 30 September 1995. The geosynchronous plane is about 35,800 km above the Earth, high enough to allow the satellites a full-disc view of the Earth. Because they stay above a fixed spot on the surface, they provide a constant vigil for the atmospheric for severe weather conditions such as tornadoes, flash floods, hail storms, and hurricanes. When these conditions develop the GOES-9 satellites are able to monitor storm development and track their movements [20].

Water vapor absorbs and reradiates electromagnetic radiation in various wavelength bands. Such infrared radiation emitted by the Earth/atmosphere and intercepted by satellites. Water vapor molecules in the atmosphere absorb outgoing terrestrial radiation in the infrared region of the electromagnetic spectrum. The AVHRR sensor on the NOAA polar orbiting satellites has two thermal channels, near 11 and 12 μm, which are designed to correct for water vapor effects when predicting sea-surface temperatures. Several investigators have employed these thermal channels in estimating total column water vapor from the AVHRR sensor (~1.1 km at nadir) in a technique referred to as the split-window technique [21]-[23].

Fig. 1 is illustrates the GOES-9 satellite images.

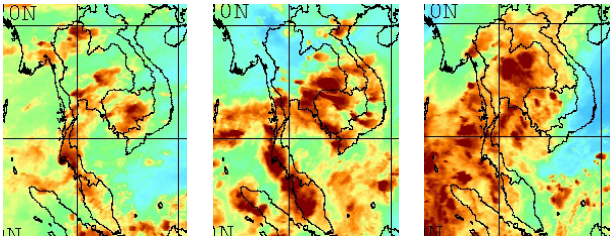

Fig. 1 Snapshots of water vapor image from the GOES-9 satellite on Thailand

III. Methodology

A. Related Work

The meteorological community has already established a number of numerical cloud analysis and forecasting systems. Much cloud analysis work has been carried out by using the empirical models and different types of satellite imaging or satellite observed data. For example, researcher proposed a cloud analysis method for rainfall forecasting in the Galician region of Spain [24]. They were applied a high-resolution non-hydrostatic numerical model to the satellite observations. They performed high-resolution cloud analysis based on statistical threshold of satellite imaging and numerical modeling [25].

However, rather than using image processing techniques to handle satellite images, they were treated and handled as ordinary data. Although this method works very well on many problems and has wide application, it is difficult to integrate spatial information and the intrinsic spatial correlations between the image pixels and the observed data values, in order to build an empirical model for the specific cloud analysis problems with spatial correlation considerations.

Although it is possible to build an empirical model in some cases, the unmanageable complexity and inadequate understanding may impede its wide application. Apart from the numerical methods, an alternative means can be chosen, according to the specific problem definition that considers spatial relationships. Researcher presented a cloud analysis method that automatically tracked clouds in meteorological satellite infrared images, based on area-overlapping analysis

[16]. They took the basic image processing and segmentation techniques to detect and track the clouds, without any assumptions of empirically physical models. From a meteorological perspective, Arnaud's approach had taken into account some basic meteorological phenomena, such as separation or merging of clouds. The method is fast and easy to compute, but the accuracy of correct cloud tracking is comparatively low, which affects its reliability when used for cloud analysis.

B. Image Processing

Water vapor images are defined as a two-dimensional function, $f(x, y)$, where x and y are spatial (plane) coordinates, and the amplitude of f at any pair of coordinates (x, y) is called the intensity or grey level of the image at that point. When x, y and the amplitude values of f are all finite, discrete quantities, we call the image a digital image. The file of digital image processing refers to processing digital images by mean of a digital computer [26]. A digital image results from a sampling of water vapor is produces a finite 2D array of values uniformly distributed over the field of view, while the brightness is restricts the sample values to a finite integer range. These necessary operations convert real-world analogue sensory data to a form suitable for computer processing and storage.

Water vapor data from GOES-9 were obtained from IR sensors, which came in 0 to 255 values. Water vapor data were then transformed to RGB colors by Naval Department, USA, in JPEG format. We downloaded the vapor maps from the navy website to our local archive automatically at half an hour intervals. After that we were read and wrote of these common image formats of water vapor data from GOES-9 satellite and store in one of the computer supported image formats [27]. The RGB (red, green, blue) color scheme of water vapor is just one of many color representation methods used in practice. The three so-called primary colors are combined (added) in various proportions to produce a composite, full-color image.

For image processing applications, it is often useful to decouple the color information from luminance. The HSV (hue, saturation, value) model has this property. Hue represents the dominant color as seen by an observer, saturation refers to the amount of dilution of the color with white light, and value defines the average brightness. The luminance component may, therefore, be processed independently of the image's color information.

When processing color images, we desired to change the color format of the image. Color format conversions were implemented as point operations. The RGB color was converted to returns a three-channel image given specifies real colors in terms of hue, saturation and brightness, each between 0 and 1. Then, we were used image processing technique transform hue of three-channel HSV color specification to single channel monochrome image that given raw image data. This monochrome raw image data had a range between 0 and 1. We were used point transformations technique convert the raw image data to 0 to 255 values.

A monochrome digital image $f(x, y)$ is a 2D array of luminance (brightness) values (1).

$$f(x,y) = \begin{pmatrix} f(0,0) & f(0,1) & \dots & f(0,N-1) \\ f(1,0) & f(1,1). & & f(1,N-1) \\ \vdots & & \ddots & \vdots \\ f(M-1,0) & f(M-1,1) & \cdots & f(M-1,N-1) \end{pmatrix} \quad (1)$$

With $f(x, y) \in Z$ where Z was the domain of the integers, and $0 \le f(x, y) \le L-1$, where typically $L = 256$. Each element of the array was called a pixel (i.e. picture element). Values in this range can be efficiently represented by 8 binary digits (note that $2^8 = 256$) and therefore, each pixel occupied one byte in memory. Total storage requirements for an image were therefore of the order of M x N bytes, where M and N were the number of rows and columns in the image arrays.

The water vapor map is a two-dimensional geographic coordinate system. We transformed the plane coordinates (east and north or x, y) to geographic coordinates (longitude and latitude). Then it was deducted of the scale map, because the real earth's shape is irregular [28]. Some information was lost in the first step of satellite products, in which an approximating, regular model is chosen. The scale was considered to be part of transforming plane coordinates to geographic coordinates. We used interpolating computational technique transform plan coordinates of water vapor image to geographic coordinates. The images were randomly opened to preview the monochrome images, which is illustrate in Fig. 2.

We extracted the pixel value from monochrome grayscale images. The method was an automatic extracted pixel value data from the satellite image sequence. The data covers the time period from January to December 2004 that it is about 17,568 images in total process. The pixel value was extracted on water vapor image specify geographic coordinates from the rain gauge locations of number rainfall from TMD. It was automatic contribution geographic coordinates of rain gauge locations over water vapor images. Besides we were got pixel value form monochrome grayscale images, we were extracted date and time from file name of water vapor image. The spatial and temporal data of pixel value was integrated the intrinsic spatial correlations between the image information and the observed rainfall data values.

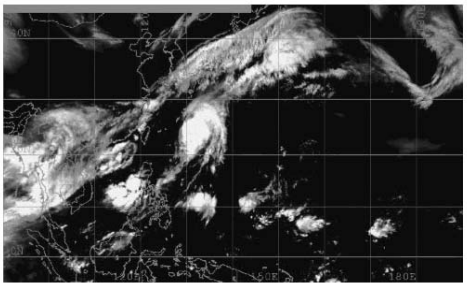

Fig. 2 A monochrome digital image

Rainfall occurred in the short time scales (generally less than 3 hours) over small spatial scales. Therefore, 48 monochrome images (24 hrs) were used for number daily rainfall from TMD. PVI was constructed by integrating all 48 images using mean and total pixel value technique. An image was designed to search the qualified pixels in the satellite images, whose TMD values satisfy. This was followed by a general data analysis process, which aimed to segment the remaining qualified pixels image into several different clusters.

If there was a high amount of water vapor in all 48 images, PVI would be high value. The high PVI is means a high probability of rainfalls in 24 hours. Each image was transformed to pixel with a value ranging from 0-255. It contained only principal grey-level regions. The method can integrate spatial information and the intrinsic spatial correlations between the image pixels and the observed data values, in order to build an empirical model for the specific cloud analysis problems with spatial correlation considerations.

The PVI is achieving accurate identification and correct detecting of water vapor from the remote sensing image sequences which is over the rain gauge locations from TMD. It provides the indispensable premise for meteorologists to make further forecasts on weather events. Since the satellite image data are spatial temporal, we need first identify and track water vapor from the entire image sequences correctly and efficiently, and then make the necessary characterization of the PVI by extracting meteorological features associated with them. To address this issue, we propose a fast detecting and characterization method of water vapor according to their feature correspondences, derived from the meteorological satellite image sequences. The method is based on the fact that in a relatively small time-span. The pixel value is progressive and detectable, which guarantees a relatively similar area and texture in two consecutive satellite images.

IV. Experimental Results

The mathematical model was obtained form a least-square fit to a list of data as a linear combination of the specified basis functions. The fit function was giving a list of commonly required diagnostics such as the coefficient of determination R squared, the analysis of variance table ANOVA Table, and the mean squared error estimated variance. The output of regression functions could be controlled so that only needed information was produced. The basic functions f_i specify the predictors as functions of the independent variables. The resulting model for the response variable is $y_i = \beta_1 f_i + \beta_2 f_{2i} + ... + \beta_p f_{pi} + e_i$, where y_i is the i^{th} response, f_{ij} is the j^{th} basis function evaluated at the i^{th} observation, and e_i is the i^{th} statistical error.

Estimates of the coefficients $\beta_1,...,\beta_p$ are calculated to minimize $\sum_i e_i^2$, the error or residual sum of squares. For example, simple linear regression is accomplished by defining the basic functions as $f_1 = 1$ and $f_2 = x$, in which case β_1 and β_2 are found to minimize $\sum_i [y_i - (\beta_1 + \beta_1 x_i)]^2$.

ANOVA able, a table for analysis of variance, provides a comparison of the given model to a smaller one including only a constant term. The table includes the degrees of freedom, the sum of squares and the mean squares due to the model (in the row labeled model) and due to the residuals (in the row labeled error). The residual mean square is also available in estimated variance, and is calculated by dividing the residual sum of squares by its degrees of freedom. The *F*-test compares the two models using the ratio of their mean squares. If the value of *F* is large, the null hypothesis supporting the smaller model is rejected.

To evaluate the importance of each basis function, we can get information about the parameter estimates from the parameter table. This table includes the estimates, their standard errors, and *t*-statistics for testing whether each parameter is zero. The *p*-values are calculated by comparing the obtained statistic to the *t* distribution with *n-p* degrees of freedom, where *n* is the sample size and *p* is the number of predictors. Confidence intervals for the parameter estimates, also based on the *t* distribution. We can be specified parameter confidence region the ellipsoidal joint confidence region of all fit parameters associated with basic functions $\{f_{i1}, f_{i2},...\}$, a subset of the complete set of basic functions. Fig. 3 illustrates the joint 95% confidence region of the regression parameters.

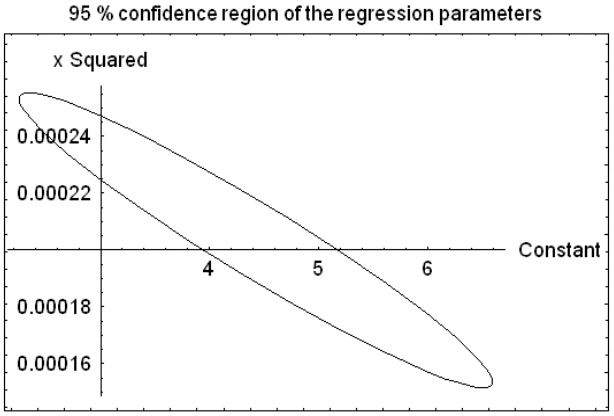

Fig. 3 This is the joint 95% confidence region of the regression parameters from model $y_i = \beta_0 + \beta_1 x_i + e_i$

The square of the multiple correlation coefficients is called the coefficient of determination R^2, and is given by the ratio of the model sum of squares to the total sum of squares. It is a summary statistic that describes the relationship between the predictors and the response variable. Adjusted R squared is defined as $\bar{R}^2 = 1 - (\frac{n-1}{n-p})(1-R^2)$, and gives an adjusted value that we can use to compare subsequent subsets of models. The coefficient of variation is given by the ratio of the residual root mean square to the mean of the response variable. If the response is strictly positive, this is sometimes used to measure the relative magnitude of error variation.

We have carried out experiments to evaluate PVI method with the amount of number rainfall proposed in the paper. We compared our PVI approach with the area-overlapping locations of number rainfall from TMD. We used the linear regression to examine the association between the averaged pixel value of daily water vapor images and the amount of daily rainfall (mm). The averaged pixel value of daily water vapor images was positively associated with the amount of daily rainfall.

The F-test using the ratio of their mean squares which the value of F was large and P lesser than 0.001(F = 92.1516, P<0.001). The null hypothesis supporting the model was rejected (Table I). This means that when we have a high averaged pixel value of daily water vapor data, we will also have a high amount of daily rainfall. This suggests that the amount of averaged pixel values can be used as an indicator of raining events. There are some positive associations between pixel values of daily water vapor images and the amount of daily rainfall at each rain-gauge station throughout Thailand.

TABLE I
THE REGRESSION OUTPUT FOR FITTING THE MODEL $y_i = \beta_0 + \beta_1 x_i + e_i$

Parameter	Estimate	SE	T Stat	P Value
Constant	4.42385	0.88633	4.9912	0
x Squared	0.0002	0.00002	9.59956	0

R Squared	Adjust R Squared	Estimated Variance
0.0175388	0.0173485	328.159

ANOVA	DF	Sum Of Sq	Mean Sq	F Ratio	P Value
Model	1	30240.4	30240.4	92.1516	0
Error	5162	0.00000169	328.1		
Total	5163	0.00000172			

This means that when we have a high averaged pixel value of daily water vapor data, we will also have a high amount of daily rainfall (Fig. 4). This suggests that the amount of averaged pixel values can be used as an indicator of raining events. There are some positive associations between pixel values of daily water vapor images and the amount of daily rainfall at each rain-gauge station throughout Thailand.

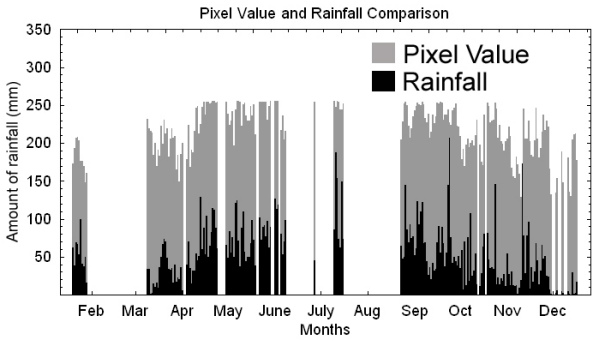

Fig. 4 The association between the averaged pixel value of daily water vapor images and the amount of daily rainfall (mm) in Thailand from TMD

The mathematical model was an abstract model that used mathematical language to describe the behavior of a system. PVI mathematical consider a pixel value of water vapor image which describes an amount of daily rainfall. It was modeled by a function $y = 0.000203415x^2 + 4.42385$ gave it an amount of daily rainfall in Thailand.

V. CONCLUSION

Grayscale images are distinct from black-and-white images, in which the context of computer imaging are images with only two colors, black and white; grayscale images have many shades of gray in between. In most contexts other than digital imaging, however, the term "black and white" is used in place of "grayscale"; for example, photography in shades of gray is typically called "black-and-white photography". The term monochromatic in some digital imaging contexts is synonymous with grayscale, and in some contexts synonymous with black-and-white. Grayscale images are often the result of measuring the intensity of light at each pixel in a single band of the electromagnetic spectrum (e.g. visible light). Grayscale images intended for visual display are typically stored with 8 bits per sampled pixel, which allows 256 intensities (i.e., shades of gray) to be recorded, typically on a non-linear scale. The accuracy provided by this format is barely sufficient to avoid visible banding artifacts, but very convenient for programming. Technical uses (e.g. in remote sensing applications) often require more levels, to make full use of the sensor accuracy (typically 10 or 12 bits per sample) and to guard against round off errors in computations. Sixteen bits per sample (65,536 levels) appears to be a popular choice for such uses.

PVI is another method that can be used for approximating the amount of daily rainfall from water vapor data from GOES-9 satellite. Image processing applications is often useful to decouple the color information from luminance. The HSV model has this property. Hue represents the dominant color as seen by an observer, saturation refers to the amount of dilution of the color with white light, and value defines the average brightness. The luminance component may, therefore, be processed independently of the image's color information.

We desired to change the color format of the image. Color format conversions were implemented as point operations. The RGB color was converted to returns a three-channel image given specifies real colors in terms of hue, saturation and brightness, each between 0 and 1. Then, we used image processing technique transform hue of three-channel HSV color specification to single channel monochrome image that given raw image data. This monochrome raw image data had a range between 0 and 1. The final image was used point transformations technique convert the raw image data to 0 to 255 values.

The PVI was extracted pixel value from monochrome image. The monochrome images were given grayscale digital image. It was an image in which the value of each pixel is a single sample. Displayed images of this sort were typically composed of shades of gray, varying from black at the weakest intensity to white at the strongest, though in principle the samples could be displayed as shades of any color, or even coded with various colors for different intensities. Characteristic of high amount water vapor on monochrome images could detect with black shade of images. Also, the contour and grid line of map was black shade similar high

amount of water vapor on monochrome images. There were few spatial data available on locations of number rainfall from TMD that overlapping on contour line of geographic map and grid of geographic coordinates. Some information of water vapor pixel value was failed to spot over contour and grid line of map. We were used a nearest pixel value replace some pixel lost information.

Besides, there are associated between the averaged pixel value of daily water vapor images and the amount of daily rainfall. Therefore, the pixel value of water vapor is a new way to predict the raining events. Then in the future, we can use these data to predict raining season in each areas. Moreover, this technique can be used to study climate change in term of anomalies in the amount of water vapor data because our results will provide a more accurate estimation of climate change and more data points because we could estimate the water vapor data every half an hour.

However, there are some limitations of this current technique. This technique depends on a real time availability of GOES-9 satellites data. Then, if the Internet is down or not reliable, downloading the GOES-9 satellite data will not be possible and satellite data, that are already downloaded, may be corrupted. This application requires high bandwidth of the Internet connection. Another limitation is the resolution of the on-board satellite sensors. For current GOES-9 satellites, the resolution is somewhat at mesoscale, so it is not possible to pinpoint a small size. Finally, at the time of doing this research, we have very limited access to data from Thai meteorological department to validate our technique. These data are rain gauge collected data from 75 stations.

In the future, this technique should be modified to use for prediction a drought risk area as an inverse function. NASA is launching a CloudSat satellite that would be closely related to this work. Data from this mission should also be used to fine tune of this technique.

ACKNOWLEDGMENTS

The authors thank Thailand Meteorological Department for their supporting the amount of daily rainfall at each rain-gauge station in Thailand. The authors are also grateful to the editors and reviewers for their valuable comments and suggestions on this manuscript.

REFERENCES

[1] C. Divjak and J. Conachy. (2001, Sep 4). "Flood tragedy in Thailand linked to deforestation," *World Socialist Web Site*. [Online]. Available: http://www.wsws.org/articles/ 2001/sep2001/thai-s04.shtml.

[2] G.R. Brakenridge and E. Anderson. (2002, Jan 25). "2001 Global Register of Extreme Flood Events," *Dartmouth Flood Observatory.* [Online]. Available: http://www.dartmouth.edu/~floods/Archives/2001sum.htm

[3] British Broadcasting Corporation. (2001, Aug 12). "Thailand floods kill 70," *BBC News*. [Online]. Available: http://www.wsws.org/articles/2001/sep2001/ thai-s04.shtml.

[4] M. D. Errico and G. Fasano, "Design of interferometric and bistatic mission phases of COSMO/SkyMed constellation," *Acta Astronautica.*, submitted for publication.

[5] R. Lucas, A. Rowlands, A. Brown, S. Keyworth and Bunting, P. "Rule-based classification of multi-temporal satellite imagery for habitat and agricultural land cover mapping," *ISPRS J. of Photogrammetry and Remote Sensing*, vol. 62, pp. 165-185, 2007.

[6] L. Vescovo and D. Gianelle, "Using the MIR bands in vegetation indices for the estimation of grasslands biophysical parameters from satellite remote sensing in the Alps region of Trentino (Italy)," *Advances In Space Research*., submitted for publication.

[7] S. Boussetta, T. Koike, K. Yang, T. Graf and M. Pathmathevan, "Development of a coupled land-atmosphere satellite data assimilation system for improved local atmospheric simulations," *Remote Sensing of Env*., submitted for publication.

[8] J. I. Fisher and J. F. Mustard, "Cross-scalar satellite phenology from ground, Landsat, and MODIS data," *Remote Sensing of Env.*, vol. 109, pp. 261-273, 2007.

[9] R. Houze, B. Smull and P. Dodge, "Mesoscale organization of springtime rainstorms in Oklahoma," *Monthly Weather Review*, vol. 18 (3), 613-654, 1990.

[10] K. Meyer, P. Yang and B. C. Gao, "Tropical ice cloud optical depth, ice water path, and frequency fields inferred from the MODIS level-3 data," *Atmospheric Research*, vol. 85, pp. 171-182, 2007.

[11] M. Bonazountasa, D. Kallidromitoub, P. Kassomenosc and N. Passasd, "A decision support system for managing forest fire casualties," *J. of Env. Management*, vol. 84, pp. 412-418, 2007.

[12] H. Feidasa, T. Kontosa, N. Soulakellisa and K. Lagouvardosb, "A GIS tool for the evaluation of the precipitation forecasts of a numerical weather prediction model using satellite data," *Computers and Geosciences*, vol. 33, pp. 989-1007, 2007.

[13] M. L. Marconi, "A kinetic model of Ganymede's atmosphere," *Icarus*, vol. 190, pp. 155-174. 2007.

[14] M. Pardé, K. Goïta and A. Royer, "Inversion of a passive microwave snow emission model for water equivalent estimation using airborne and satellite data," *Remote Sensing of Env.*, submitted for publication.

[15] N. H. Wong, S. K. Jusuf, A. A. L. Win, H. K. Thu, T. S. Negara and W. Xuchao, "Environmental study of the impact of greenery in an institutional campus in the tropics," *Building and Env.*, vol. 42, pp. 2949-2970, 2007.

[16] Y. Arnaud, M. Desbios and J. Maizi, "Automatic tracking and characterization of African convective systems on meteosat pictures," *J. of App. Meteorology.*, vol. 31 (5), pp. 443-453, 1992.

[17] H. Xiaoa and Q. Wengb, "The impact of land use and land cover changes on land surface temperature in a karst area of China," *J. of Env. Management.*, vol. 85, pp. 245-257, 2007.

[18] J. Guo, G. Fu, Z. Li, L. Shao, Y. Duan and J. Wang, "Analyses and numerical modeling of a polar low over the Japan Sea on 19 December 2003," *Atmospheric Research*, vol. 85, pp. 395-412, 2007.

[19] G. P. Ellrod, R.V. Achutuni, J.M. Daniels, E.M. Prins and J.P. Nelson, "An assessment of GOES-8 imager data quality," *Bulletin American Meteorological Society*, vol. 79, pp. 2509-2526, 1998.

[20] NASA-GSFC and NOAA, 2007. "GOES-J Status," Available:http://rsd.gsfc.nasa.gov/goes/text/goesjstatus.html

[21] G. Dalu, "Satellite remote sensing of atmospheric water vapor," *Inter. J. of Remote Sensing*, vol. 7, pp. 1089-1097, 1986.

[22] T. J. Kleespies and L. M. McMillin, "Retrieval of precipitable water from observations in the split window over varying surface temperatures," *J. of App. Meteorology*, vol. 29, pp. 851-862, 1990.

[23] J. C. Roger and E.F. Vermote, "A method to retrieve the reflectivity signature at 3.75µm from AVHRR Data," *Remote Sensing of the Env.*, vol. 64, pp. 103-114, 1998.

[24] M.J. Souto, C.F. Balseiro, V. Pe´rez-Mun˜uzuri, M. Xue, and K. Brewster, "Impact of cloud analysis on numerical weather prediction in the Galician region of Spain," *J. of App. Meteorology*, vol. 42, pp. 129-140, 2003.

[25] M.P. Plonski, G. Gustafson, B. Shaw, B. Thomas and M. Wonsick, "High resolution cloud analysis and forecast system," in *Proc. of the 10th Conf. on Satellite. Meteorology and Ocean of American. Meteorology Soc.*, Long Beach, CA, USA, 2000. pp. 114-117.

[26] R. C. Gonzalez and R.E. Woods, "Image Segmentation," in *Digital Image Processing*, 2nd ed. W. M. Euclid, Ed. Pearson Education (Singapore) Pte. Ltd., Indian Branch, 2002, pp. 567-636.

[27] S. Wolfram, "The Mathematica Book," *Book News*, 5th ed. Oregon. 2004.

[28] S. I. Zhilin, "Simple method for outlier detection in fitting experimental data under interval error," *Chemometrics and Intelligent Lab. Systems*, vol. 88, pp. 60-68. 2007.